Detailed analysis of the acoustic properties of a permeable membrane

Sakagami, Kimihiro
Kiyama, Masakazu
Morimoto, Masayuki
Takahashi, Daiji

(Citation)
Applied Acoustics,54(2):93-111

(Issue Date)
1998-06

(Resource Type)
journal article

(Version)
Accepted Manuscript

(URL)
https://hdl.handle.net/20.500.14094/90000854

Detailed analysis of the acoustic properties of a permeable membrane

Kimihiro Sakagami

Environmental Acoustics Laboratory, Faculty of Engineering, Kobe University, Rokko, Nada, Kobe, 657 Japan

Masakazu Kiyama

Graduate School of Science and Technology, Kobe University, Rokko, Nada, Kobe, 657 Japan, and Nippon Sheet Glass Co., Ltd., Osaka, 531 Japan

Masayuki Morimoto

Environmental Acoustics Laboratory, Faculty of Engineering, Kobe University, Rokko, Nada, Kobe, 657 Japan

&

Daiji Takahashi

Department of Architecture, Faculty of Engineering, Kyoto University, Yoshida-Hommachi, Sakyo, Kyoto, Japan

ABSTRACT

A detailed analysis is carried out to clarify the mechanisms governing the acoustic performance of a permeable membrane and the effects of various material parameters. For this purpose, the theoretical solutions for the reflected and transmitted sound fields by an infinite permeable membrane which have been derived in a previous paper [J. Acoust. Soc. Am. **99**, 3003-3009 (1996)] are approximated to obtain simple expressions for normal incidence absorption and transmission coefficients. An electrical circuit analogy is employed for a detailed analysis in which the particle velocity is separated into two components, i.e. the mass and the permeability, which is helpful in understanding their contributions to the acoustic properties of the permeable membrane. These considerations are aimed at demonstrating the effects of the parameters on the acoustic properties as well as explaining the following particular phenomena which are observed in the acoustic properties of a permeable membrane: the decrease of the sound energy absorbed in the structure at low frequencies and the increase of transmission loss at low frequencies due to the permeability. The optimal value of flow resistance for the most effective absorption is also obtained from those solutions.

1 Introduction

Membranes are becoming more widely used as both building and acoustic materials. As a building material they are usually incorporated as an integrated construction of the roof and ceiling in a membrane-structure building[1]. There have also been some attempts to use membranes as acoustic materials, for example, as sound absorbers[2], removable sound reflectors in auditoria[3] and sound insulating materials[4]. The authors have derived theoretical results for the sound reflectivity of an impermeable membrane[5], which can be applied to a sound reflector of the type mentioned above or a single-leaf roof in a building.

Some types of membrane which are used as a building material have some degree of acoustic permeability. For these membranes the permeability must be taken into account when sound fields involving boundaries of this type are analysed. The basic approach in determining the acoustic properties of a permeable membrane is presented in Ref [6], in which Pierce analysed the sound transmission through porous blankets considering the flow resistance and the mass impedance. In a previous paper, the authors have established a more sophisticated approach to analyse the acoustic properties of a permeable membrane[7]. The theory is formulated by coupling a Helmholtz integral for the sound field and an equation of motion for the membrane including its mass as well as tension so that it can be applied to analyses of sound reflection, absorption and transmission under oblique incidence of a plane sound wave. Some numerical examples of acoustic properties calculated by the theory, which are field-incidence-averaged values, have been briefly considered in the previous paper. These illustrate the effects of the parameters: tension, mass and flow resistance of the membrane. It has become clear that the acoustic properties of a membrane can strongly be affected by changes in its permeability as well as its mass. However, these properties were not discussed in detail, and some particular trends observed in the results have been left unexplained in the paper. Therefore, the aim of the present paper is to explore further the acoustic properties of a permeable membrane, as a supplement to the previous paper[7]. In this study, special consideration will be given to the acoustic properties at low frequencies which show characteristic behaviour. For this purpose, the general solutions given in [7], which are rather complicated, are simplified by restricting them to a normal incidence case in most parts of this study. The tension will be neglected because its effect has been found to be small and less significant than the effects of the other parameters.

2 Sound absorption and transmission of a single-leaf permeable membrane

2.1 Theoretical solutions for the sound pressures reflected and transmitted by a single-leaf permeable membrane

Consider the sound field around a permeable membrane of infinite extent, lying in the z=0 plane, shown in Fig 1, which is characterised by its surface density m, tension T and flow resistivity R. The membrane has the thickness h and the flow resistance is Rh. The incident sound wave is a plane wave with a unit pressure amplitude. The angle of incidence is denoted by θ.

Using a Helmholtz integral for the two-dimensional sound field coupled with the equation of motion of the membrane, in which the flow resistance is included as a boundary condition, closed form solutions for the reflected and the transmitted pressures, p_r and p_t, respectively, are given as follows [7]:

$$p_r(x,z) = \frac{\cos\theta + i\rho_0\omega^2 F(k_0 \sin\theta)\cos\theta}{\cos\theta + 2A_M}\exp[ik_0(x\sin\theta - z\cos\theta)] \quad , \tag{1}$$

$$p_t(x,z) = \frac{2A_M - i\rho_0\omega^2 F(k_0 \sin\theta)\cos\theta}{\cos\theta + 2A_M}\exp[ik_0(x\sin\theta + z\cos\theta)] \quad , \tag{2}$$

where

$$F(k_0 \sin\theta) = \frac{4\pi U(k_0 \sin\theta)}{2k_0 A_M + k_0\cos\theta - 4\pi i\rho_0\omega^2 U(k_0 \sin\theta)}, \tag{3}$$

and $U(k_0\sin\theta)=[2\pi T(k_0^2\sin^2\theta - m\omega^2/T)]^{-1}$, with ρ_0 is the air density, k_0 the acoustic wavenumber ($=\omega/c_0$, ω the angular frequency and c_0 the sound speed in the air) and $A_M=\rho_0 c_0/Rh$. The time dependence of $\exp(-i\omega t)$ is suppressed throughout.

2.2 Absorption and transmission coefficients

Since in the above solutions, Eqs (1)-(3), the incident sound wave is assumed to have a unit pressure amplitude, the oblique incidence absorption and transmission coefficients, α_θ and τ_θ, respectively, are obtained as:

$$\alpha_\theta = 1 - |p_r|^2 \tag{4}$$

and

$$\tau_\theta = |p_t|^2 . \tag{5}$$

Equations (4) and (5) have rather complicated form and are not practical for detailed analyses, however, considerable simplification can be made if they are restricted to normal incidence, which does not lose the generality of discussion, and the tension T which is known to have little effect is neglected. Thus the normal incidence absorption and transmission coefficients, α_n and τ_n, respectively, are derived as:

$$\alpha_n = \frac{4A_M^2 + 4A_M + 4M_M^2}{4A_M^2 + 4A_M + 4M_M^2 + 1}, \tag{6}$$

$$\tau_n = \frac{4A_M^2 + 4M_M^2}{4A_M^2 + 4A_M + 4M_M^2 + 1}, \tag{7}$$

where $M_M = \rho_0 c_0 / \omega m$.

The normal acoustic impedance, defined as the ratio of the differential pressure between the two sides of the membrane to the particle velocity in this case, is

$$Z = \frac{1}{\frac{1}{Rh} - \frac{1}{i\omega m}}. \tag{8}$$

Note that the absorption coefficient cannot be correctly evaluated if this is substituted into the well-known formula

$$\alpha^* = \frac{4\rho_0 c_0 \,\mathrm{Re}[Z]}{|Z|^2 + 2\rho_0 c_0 \,\mathrm{Re}[Z] + (\rho_0 c_0)^2}, \tag{9}$$

since the absorption coefficient α includes the energy transmitted through the membrane, that is described by the transmission coefficient τ. The difference between α and τ, $\alpha-\tau$ which represents the energy actually dissipated in the structure, is used throughout this paper in order to evaluate the absorption characteristics of membranes.

3 Discussion

3.1 Effect of flow resistance

Examples of calculated results of the normal incidence coefficients α_n, τ_n and $\alpha_n-\tau_n$ for various values of flow resistance Rh are shown in Fig 2. As Rh increases, α_n monotonically decreases. When the flow resistance is low, Rh=100 MKSrayl in this example, the absorption coefficient α_n is about 1.0 at all frequencies. On the other hand, for greater values of Rh, α_n monotonically decreases with increasing frequency to converge on a certain value at high frequencies. The value at high frequencies on which α_n converges is the limit in Eq (6), as $\omega m \to \infty$, which is

$$\alpha_n \to \frac{4(\rho_0 c_0)^2 + 4\rho_0 c_0 Rh}{(2\rho_0 c_0 + Rh)^2}. \tag{10}$$

In the case of an impermeable material which complies with the mass-law relation, the transmission coefficient τ_n generally decreases to converge on zero as frequency increases. However, a permeable membrane does not necessarily follow the mass-law relation, so that although τ_n decreases with increasing frequency, it does not converge on zero but on a certain non-zero value that is the limit of τ_n, Eq (7) as $\omega m \to \infty$, which is

$$\tau_n \to \frac{4(\rho_0 c_0)^2}{(2\rho_0 c_0 + Rh)^2}. \tag{11}$$

The difference between these two coefficients, $\alpha_n - \tau_n$, is zero for all frequencies at the extreme values of flow resistance (*Rh*). In the case of extremely low flow resistance, almost all energy is transmitted through the membrane. On the contrary, in the case of very high values of *Rh*, the membrane becomes almost impermeable. As a result α_n and τ_n become approximately equal. In the case when $Rh=10^4$ MKSrayl, $\alpha_n - \tau_n$ monotonically increases as frequency increases. The value at which $\alpha_n - \tau_n$ converges depends on *Rh*, and becomes the largest when $Rh=10^3$ MKSrayl. This suggests that there is an optimal value of *Rh* which maximises $\alpha_n - \tau_n$, as is the case of other porous materials. The detailed discussion of this optimal value will be given later. The limit of $\alpha_n - \tau_n$ as $\omega m \to \infty$, to which $\alpha_n - \tau_n$ converges at high frequencies, is obtained by taking the difference of Eqs (10) and (11):

$$\alpha_n - \tau_n \to \frac{4\rho_0 c_0 Rh}{(2\rho_0 c_0 + Rh)^2}. \tag{12}$$

Equations (10)-(12) show that α_n, τ_n and $\alpha_n - \tau_n$ at high frequencies are determined by *Rh* only.

3.2 Effect of mass

Calculated examples of α_n, τ_n and $\alpha_n - \tau_n$ for different values of *m* are shown in Fig 3. The effect of the mass of the membrane appears mainly at low frequencies, whereas that of flow resistance appears at high frequencies. The values of α_n, τ_n and $\alpha_n - \tau_n$ at high frequencies are almost constant and converge on the values given by Eqs (10)-(12), even if the mass changes. Since the values given by Eqs (10)-(12) are limiting values as $\omega m \to \infty$, they are not only the limiting values for high frequencies, but also indicate the limiting values for a massive membrane, which are determined only by *Rh*. Thus, the mass has hardly any effect on the acoustic properties at high frequencies, and only *Rh* is the dominant parameter. However, if the mass increases, the properties converge to the limiting values at lower frequencies.

On the other hand, the effect of *m* is significant at low frequencies. When $m \to \infty$, all acoustic properties show constant values regardless of frequency, and they are determined by *Rh* only. Both α_n and τ_n decrease at low frequencies as *m* decreases.

The degree of increase in τ_n is greater than that in α_n. The difference between them produces the decrease of $\alpha_n - \tau_n$. This means that the decrease in the energy dissipated in the membrane reduces with decreasing *m*. This drop in $\alpha_n - \tau_n$ or the energy loss in the membrane is related to the behaviour of the real part of the membrane impedance Re[Z] at low frequencies. Calculated results for $\mathrm{Re}[Z]=Rh(\omega m)^2/[(\omega m)^2+(Rh)^2]$ are shown in Fig 4. Re[Z] is equal to *Rh*, and independent of frequency when $m \to \infty$. It decreases at low frequencies showing similar behaviour to $\alpha_n - \tau_n$ with decreasing *m*. When *m* is finite, Re[Z] monotonically decreases as frequency decreases. The more *m* decreases, the lower the frequency where the decrease starts. This trend is also similar to the behaviour of $\alpha_n - \tau_n$. Therefore, this behaviour of a permeable membrane at low frequencies appears to be caused by the decrease of resistance Re[Z] at low frequencies which is the effect of its finite mass. More detailed discussion will be found in Section 3.4.

3.3 Effect of angle of incidence

Figure 5 shows spectra of α_θ, τ_θ and $\alpha_\theta - \tau_\theta$ calculated using Eqs (1)-(5). In the case of oblique-incidence, the same features of the acoustic properties as in the normal-incidence cases are observed regardless of the angle of incidence. When the angle of incidence increases, α_θ and τ_θ increase, whereas $\alpha_\theta - \tau_\theta$ decreases. The explanation, usually given in the case of an elastic plate, for the cause of the increase of sound transmission with increasing angle of incidence is that bending waves travelling in the structure are more easily established at larger angles of incidence. However it is most unlikely to be the case for a membrane: In these examples, the effect is seen even at high frequencies where the membrane can hardly vibrate. Therefore, it is obvious that this increase of transmission cannot be explained by the increase in bending-wave effect only. When the membrane does not vibrate at all, that is $\omega m \to \infty$, from Eqs (1)-(3), the reflected and transmitted pressures, p_r and p_t, are

$$p_r = \frac{\cos\theta}{\cos\theta + 2A_M}, \tag{13}$$

$$p_t = \frac{2A_M}{\cos\theta + 2A_M}. \tag{14}$$

>From Eqs (13) and (14), α_θ, τ_θ and $\alpha_\theta - \tau_\theta$ are derived as follows:

$$\alpha_\theta = \frac{4\rho_0 c_0 Rh\cos\theta + 4(\rho_0 c_0)^2}{(Rh\cos\theta + 2\rho_0 c_0)^2}, \tag{15}$$

$$\tau_\theta = \frac{4(\rho_0 c_0)^2}{(Rh\cos\theta + 2\rho_0 c_0)^2}, \tag{16}$$

$$\alpha_\theta - \tau_\theta = \frac{4\rho_0 c_0 Rh\cos\theta}{(Rh\cos\theta + 2\rho_0 c_0)^2}. \tag{17}$$

Comparing Eqs (15)-(17) with Eqs (10)-(12) for the normal incidence case, it is found that the former are the same as the latter if *Rh* is replaced with $Rh\cos\theta$. Considering that the impedance of the permeable membrane is *Rh* for normal incidence when $m\rightarrow\infty$, it can be inferred that in oblique-incidence cases the impedance reduces to $Rh\cos\theta$. Increasing the angle of incidence gives more reduction in flow resistance by the factor of $\cos\theta$. This decrease in flow resistance gives rise to the observed increase in transmission with increasing angle of incidence.

3.4 Detailed analysis by equivalent circuit analogy

The following three characteristics will be of particular interest in this section:

(1) The drop in the energy dissipated in the membrane at low frequencies.

(2) The increase in the transmission loss at low frequencies due to permeability.

(3) The optimal value of flow resistance to give the highest absorption.

In the following analysis, the particle velocity in and around the membrane is divided into two components, the vibration velocity of the membrane v_m, which indicates the contribution of the mass to its acoustic properties, and the relative velocity $v_{Rh}=v_f-v_m$, which represents the contribution of the flow resistance to the acoustic properties. Regarding v_m and v_{Rh} as equivalent to the currents in the resistor *Rh* and in the inductor $-i\omega m$, respectively, in the equivalent circuit (Fig 6), they can be obtained as:

$$v_m = \frac{2\left\{2\rho_0 c_0 (Rh)^2 + i\omega m Rh(2\rho_0 c_0 + Rh)\right\}}{4(\rho_0 c_0 Rh)^2 + (\omega m)^2 (2\rho_0 c_0 + Rh)^2}, \tag{18}$$

$$v_{Rh} = \frac{2\left\{(\omega m)^2 (2\rho_0 c_0 + Rh) - 2i\omega m \rho_0 c_0 Rh\right\}}{4(\rho_0 c_0 Rh)^2 + (\omega m)^2 (2\rho_0 c_0 + Rh)^2}. \tag{19}$$

The entire particle velocity $v_f=v_m+v_{Rh}$ is equivalently described as the entire current in the circuit, which is

$$v_f = \frac{2\left\{2\rho_0 c_0 (Rh)^2 + (\omega m)^2 (2\rho_0 c_0 + Rh) + i\omega m (Rh)^2\right\}}{4(\rho_0 c_0 Rh)^2 + (\omega m)^2 (2\rho_0 c_0 + Rh)^2} . \tag{20}$$

A calculated example of v_f, v_m and v_{Rh} is shown in Fig 7 by a vector representation on a complex plane. The length of each arrow indicates the magnitudes of v_f, v_m and v_{Rh}. The semicircles are loci of v_f, v_m and v_{Rh} with changing frequency. From this figure, the changes in magnitude of each velocity and the contributions of v_m and v_{Rh} to v_f can be understood. The total particle velocity v_f decreases as frequency increases, and finally converges to the limit as $\omega m \to \infty$, which is

$$v_f \big|_{\omega m \to \infty} = v_{Rh} \big|_{\omega m \to \infty} = \frac{2}{Rh + 2\rho_0 c_0} . \tag{21}$$

v_{Rh} is small at low frequencies, and increases as frequency increases. Meanwhile the contribution of v_{Rh} to v_f increases, and v_{Rh} becomes the dominant contributor to v_f at high frequencies. Both v_f and v_{Rh} converge on the same value as $\omega m \to \infty$.

Conversely, v_m is great at low frequencies and decreases with increasing frequency. The contribution of v_m to v_f is great at low frequencies and becomes smaller as frequency increases, at high frequency limit $\omega m \to \infty$, it becomes zero.

3.4.1 Effect of flow resistance on internal energy loss

The analogy that the energy dissipated in the system corresponds to that consumed by the resistor *Rh* in the equivalent circuit can be employed to calculate the energy dissipated in the membrane.

In the equivalent circuit of the permeable membrane, Fig 6, the energy consumed by the resistor *Rh*, E_a can be written as

$$E_a = \frac{4Rh(\omega m)^2}{4(\rho_0 c_0 Rh)^2 + (\omega m)^2 (Rh + 2\rho_0 c_0)^2} . \tag{22}$$

If the ratio of E_a to the intensity of incident plane wave $1/\rho_0 c_0$ is taken, the result becomes the same as $\alpha_n - \tau_n$, which is

$$\alpha_n - \tau_n = \frac{4\rho_0 c_0 Rh(\omega m)^2}{4(\rho_0 c_0 Rh)^2 + (\omega m)^2 (Rh + 2\rho_0 c_0)^2} . \tag{23}$$

With this it is verified that $\alpha_n-\tau_n$ actually represents the energy dissipated in the membrane. Furthermore, E_a can be rewritten as $E_a=|v_{Rh}|^2 Rh$, therefore,

$$\alpha_n - \tau_n = \rho_0 c_0 |v_{Rh}|^2 Rh\,. \tag{24}$$

With these considerations, the decrease of $\alpha_n-\tau_n$ or the energy loss in the membrane with reducing frequency can be interpreted. As the frequency decreases, $-i\omega m$ becomes smaller, which makes v_m greater and v_{Rh} smaller. From Eq (24), if v_{Rh} decreases in this way, the energy loss, $\alpha_n-\tau_n$, decreases because Rh is constant. This can be physically interpreted as increased vibration making the flow velocity in the membrane smaller, thus reducing the energy loss.

3.4.2 Optimal value of flow resistance for higher absorption

The existence of a value which gives the largest $\alpha_n-\tau_n$ or the greatest energy loss has already been pointed out. Figure 8 shows the normal-incidence absorption and transmission coefficients, α_n and τ_n, and their difference $\alpha_n-\tau_n$ as functions of flow resistance Rh. It can be seen that the energy loss $\alpha_n-\tau_n$ achieves a maximum at a certain value of Rh which varies with frequency. These values can be obtained by solving

$$\frac{d}{d(Rh)}\left(\alpha_n - \tau_n\right) = 0$$

for Rh. The solution, which is the optimal value, is

$$Rh_o = \frac{1}{\sqrt{\left(\dfrac{1}{\omega m}\right)^2 + \left(\dfrac{1}{2\rho_0 c_0}\right)^2}} \tag{25}$$

for normal incidence. Equation (25) includes ωm so that the optimal value changes with frequency and the mass of the membrane. The optimal value decreases as frequency decreases, hence the maximum energy loss decreases by Eq (24). In Fig 8 all the curves coincide for frequencies greater than 1000 Hz. At high frequencies $(1/\omega m)\approx 0$ and $Rh_o \approx 2\rho_0 c_0$. In this case, the maximum value of $\alpha_n-\tau_n$ is 0.5, and this predicts that the energy loss caused by a permeable membrane never exceeds 0.5.

In the case of oblique incidence, a similar expression for the optimal value can be obtained from Eqs (1) and (2):

$$Rh_\theta = \frac{1}{\sqrt{\left(\dfrac{1}{T\omega \sin^2\theta / c_0 - \omega m}\right)^2 + \left(\dfrac{\cos\theta}{2\rho_0 c_0}\right)^2}}\,. \tag{26}$$

If the tension T is neglected, which is found to be reasonable in many cases [5,7], the optimal value is given as

$$Rh_\theta = \frac{1}{\sqrt{\left(\frac{1}{\omega m}\right)^2 + \left(\frac{\cos\theta}{2\rho_0 c_0}\right)^2}}. \tag{27}$$

Thus, the optimal value of Rh will be approximately $2\rho_0 c_0/\cos\theta$ at high frequencies. In this case, the maximum value of $\alpha-\tau$ is smaller than that for normal incidence.

3.4.3 Effect of flow resistance on sound transmissibility

Figure 9 shows an example of transmission loss of a permeable membrane in comparison with that of an impermeable membrane calculated using Eq (7). The transmission loss of the permeable membrane exceeds that of the impermeable membrane at low frequencies.

Rearranging Eq (18), gives the following expression:

$$v_m = \frac{2}{2\rho_0 c_0 - i\omega M}, \tag{28}$$

where $M=m(1+2\rho_0 c_0/Rh)$. Comparing this with the vibration velocity of an impermeable membrane v_{mi} which is

$$v_{mi} = v_{Rh}\big|_{Rh\to\infty} = \frac{2}{2\rho_0 c_0 - i\omega m}, \tag{29}$$

it is clear that Eq (28) takes the same form as Eq (29) replacing $-i\omega m$ with $-i\omega M$. Since M is always greater than m, Eq (28) suggests that the permeability can be described as an effective increase in the mass.

Calculated examples of v_m, v_{Rh} and v_{mi} are shown in Fig 10 for $M/m\approx 1.8$. The curve for v_m is similar to that for v_{mi} but shifted to lower frequencies by nearly one octave. In other words, the value of v_m at a certain frequency corresponds to the value of v_{mi} at a frequency approximately one octave higher.

The decrease of v_m indicates that the vibration of the membrane is suppressed by the effect of permeability, and this causes the relative velocity of the flow in the membrane, v_{Rh}, to be increased so that the energy loss becomes greater. Figure 11 has been constructed in a similar manner to Fig 7 using Eqs (18)-(20) and considering a frequency of 31.5 Hz. The loci for different values of flow resistance coincide for v_m. The magnitude of v_m, that is indicated by thin arrows in the upper half of the figure, decreases with decreasing Rh. The magnitude of v_{Rh} shows the opposite trend. The total velocity v_f

decreases when *Rh* is reduced from 1000 to 100, however, it increases when *Rh* is reduced further. This is because the impedance of the entire system becomes very small. This implies that there is a value of *Rh* at which the permeability has the greatest effect in minimising the transmissibility. The value can be found from Fig 8 (b), and the value is close to that which maximises the energy loss.

4 Conclusion

In this paper the acoustic properties of a single-leaf permeable membrane have been investigated in detail. A parametric study was made to clarify the effects of membrane parameters such as surface density and flow resistance. The effect of flow resistance appears mainly at high frequencies, whereas that of mass is significant at low frequencies. The energy loss of the permeable membrane decreases at low frequencies due to the effect of finite mass. The effect of the angle of incidence can be interpreted as an apparent reduction of flow resistance which reduces the impedance by factor of $\cos\theta$. An equivalent circuit analogy was employed to separate the contributions of mass and permeability to the acoustic properties. Two particular phenomena, the drop in energy loss and the increase in the transmission loss at low frequencies, which are typical of a permeable membrane have been explained using the results. The drop in the energy loss can be interpreted as increased vibration making the flow velocity in the membrane smaller. Flow resistance is found to have an effect equivalent to an additional mass which increases the transmission loss at low frequencies. The optimal value of flow resistance giving the most effective absorption, which is of great interest in practical applications, has also been derived by theoretical analysis and is given in Eqs (25)-(27). The optimal value of flow resistance which has the greatest effect in minimising the transmissibility has also been suggested.

Acknowledgement

The authors are indebted to Mr Koichiro Fujita for his assistance in numerical calculations. They also thank Drs David C Hothersall and Kirill V Horoshenkov at University of Bradford for their invaluable comments.

References

[1] Maekawa, Z, Acoustical design of the Kobe Port-Island Hall, Proceedings of the 12th ICA, Canada (ICA, Toronto, 1986), **vol II**, E3-6.

[2] Koga, S, Improvement of sound absorption of thin film - Studies of absorption characteristics by equivalent circuit -, J Acoust Soc Jpn(J) **52**, 92-98 (1996) (in Japanese).

[3] Strøm, S, Orchestra enclosures and stage design in multipurpose halls used for concerts, Proceedings of the 13th ICA, Yugoslavia (ICA, Belgrade, 1989), 183-186.

[4] Hashimoto, N, Katsura, M, Yasuoka, M & Fujii, H, Sound insulation of a rectangular thin membrane with additional weights, Appl Acoust **33**, 21-43 (1991).

[5] Sakagami, K, Morimoto, M & Takahashi, D, A note on acoustic reflection of an infinite membrane, Acustica **80**, 569-572 (1994).

[6] Pierce, A D, Acoustics, An Introduction to Its Physical Principles and Applications (McGraw-Hill, NY, 1981), Chaps 3-8.

[7] Takahashi, D, Sakagami, K & Morimoto, M, Acoustic properties of permeable membranes, J Acoust Soc Am **99**, 3003-3009 (1996).

Captions of figures

Figure 1 Geometry of an infinite permeable membrane: surface density, tension and flow resistivity of membrane are m, T and Rh, respectively.

Figure 2 Effect of the flow resistance Rh on the acoustic properties of a permeable membrane: m = 1.0 kg/m^2, Rh = 1 (1), 10^2 (2), 10^3 (3), 10^4 (4), ∞ (5) MKSrayl.

Figure 3 Effect of the mass m on the acoustic properties of a permeable membrane: m = 0.5 (1), 1.0 (2), 2.0 (3), 4.0 (4) kg/m^2, Rh=10^3 MKSrayl.

Figure 4 Variation of Re[Z], the resistance, of a permeable membrane due to a change in the mass: m = 0.5 (1), 1.0 (2), 2.0 (3), 4.0 (4), ∞ (5) kg/m^2.

Figure 5 Variation of α_θ (a), τ_θ (b) and $\alpha_\theta - \tau_\theta$ (c) due to a change in the angle of incidence θ. Rh = 10^3 MKSrayl, m = 1.0 kg/m^2.

Figure 6 Electrical equivalent circuit for a permeable membrane under normal incidence of a plane wave.

Figure 7 An example of the vector representation of velocity components, v_m, v_{Rh} and v_f, on a complex plane. Thin upward arrows indicate the magnitude of v_m, and thin downward ones denote that of v_{Rh} for each frequency. Thick arrows show the magnitude of v_f for each frequency. Three semicircles represent the loci of those components with changing frequency. Rh = 10^3MKSrayl, m = 1.0 kg/m^2.

Figure 8 Variation of α_n (a), τ_n (b) and $\alpha_n - \tau_n$ (c) due to a change in Rh. m = 1.0 kg/m^2. Note that the curves for the frequencies higher than 500 Hz are overlapped in (c).

Figure 9 An example of the transmission losses of permeable and impermeable membranes. Rh = 10^3 MKSrayl, m = 1.0 kg/m^2.

Figure 10 Comparison of relative magnitude of velocity components due to mass, v_m, and flow resistance, v_{Rh}, in a permeable membrane, with that of an impermeable membrane, v_{mi}, (a) real and (b) imaginary parts, and (c) absolute values. Rh = 10^3 MKSrayl, m = 1.0 kg/m^2.

Figure 11 Variation of the magnitude and the loci of the velocity components, v_m, v_{Rh} and vf, due to a change in the flow resistance: Rh=1, 100 and 1000 MKSrayl. m = 1.0 kg/m^2. Frequency is 31.5 Hz.

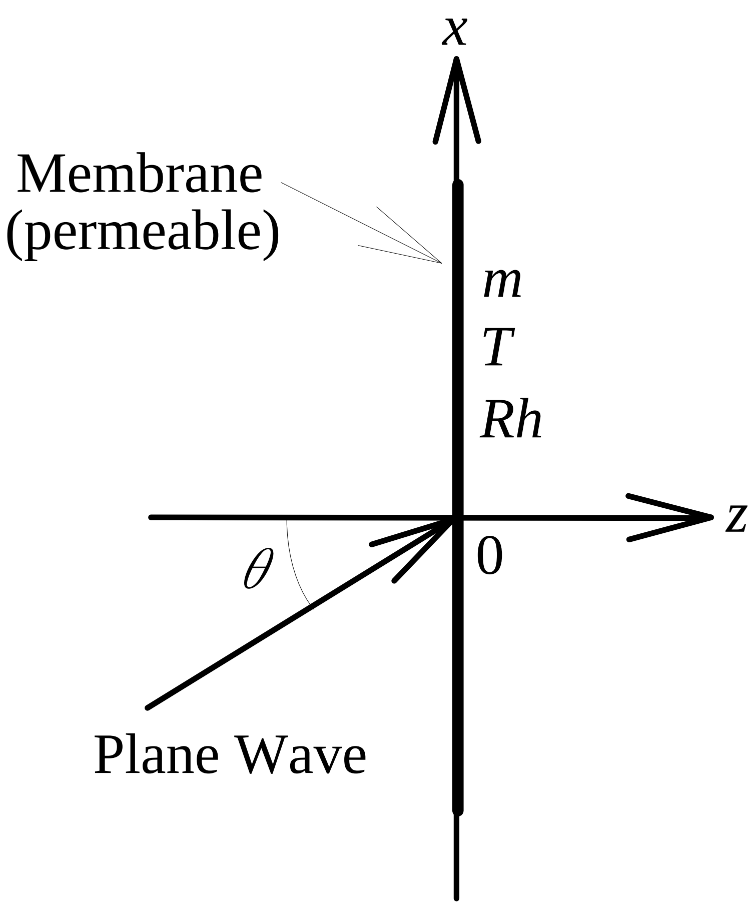

K Sakagami, et al. Detailed analysis of acoustic properties of a permeable membrane

Fig. 1

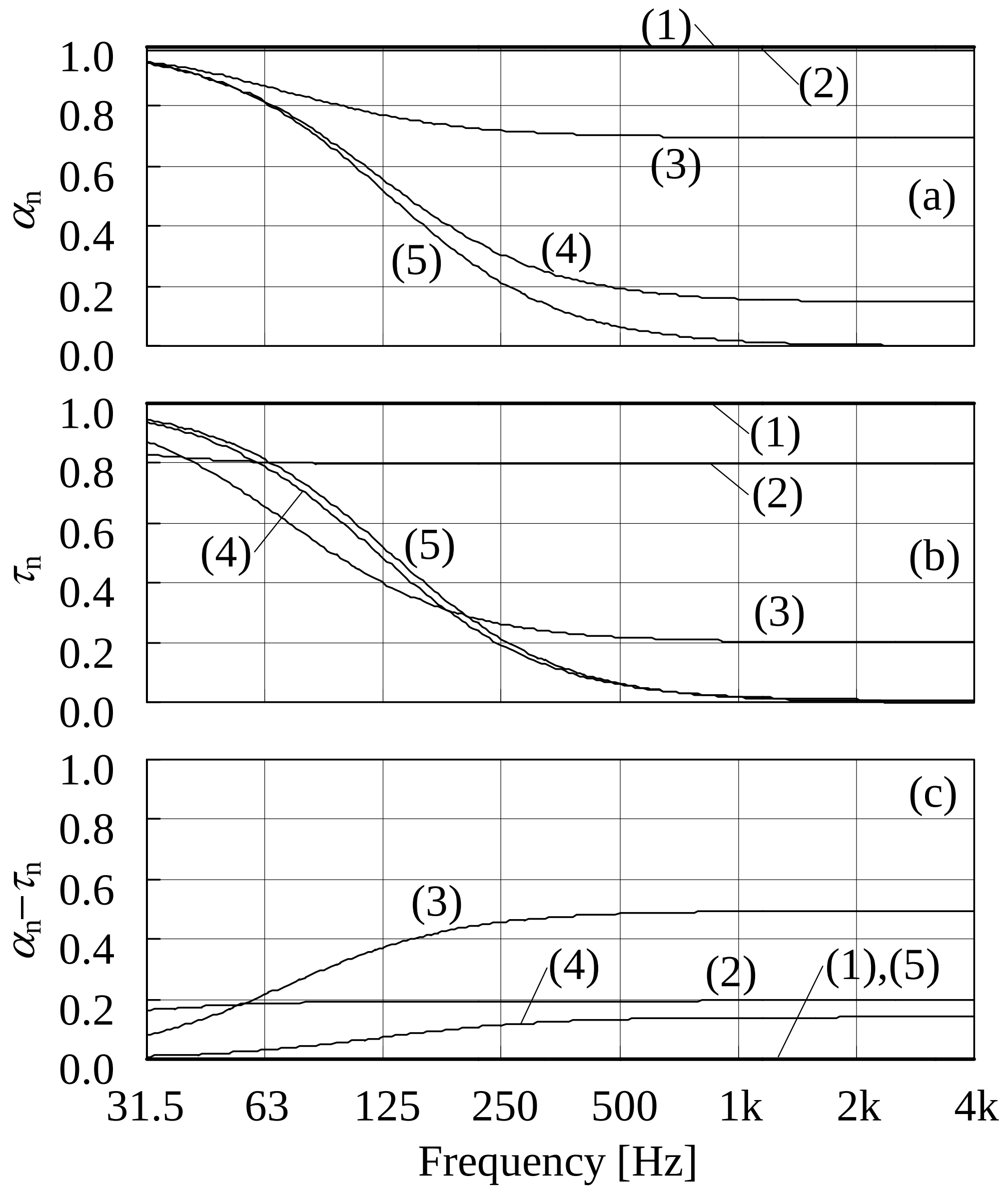

K Sakagami, et al. Detailed analysis of acoustic properties of a permeable membrane

Fig. 2

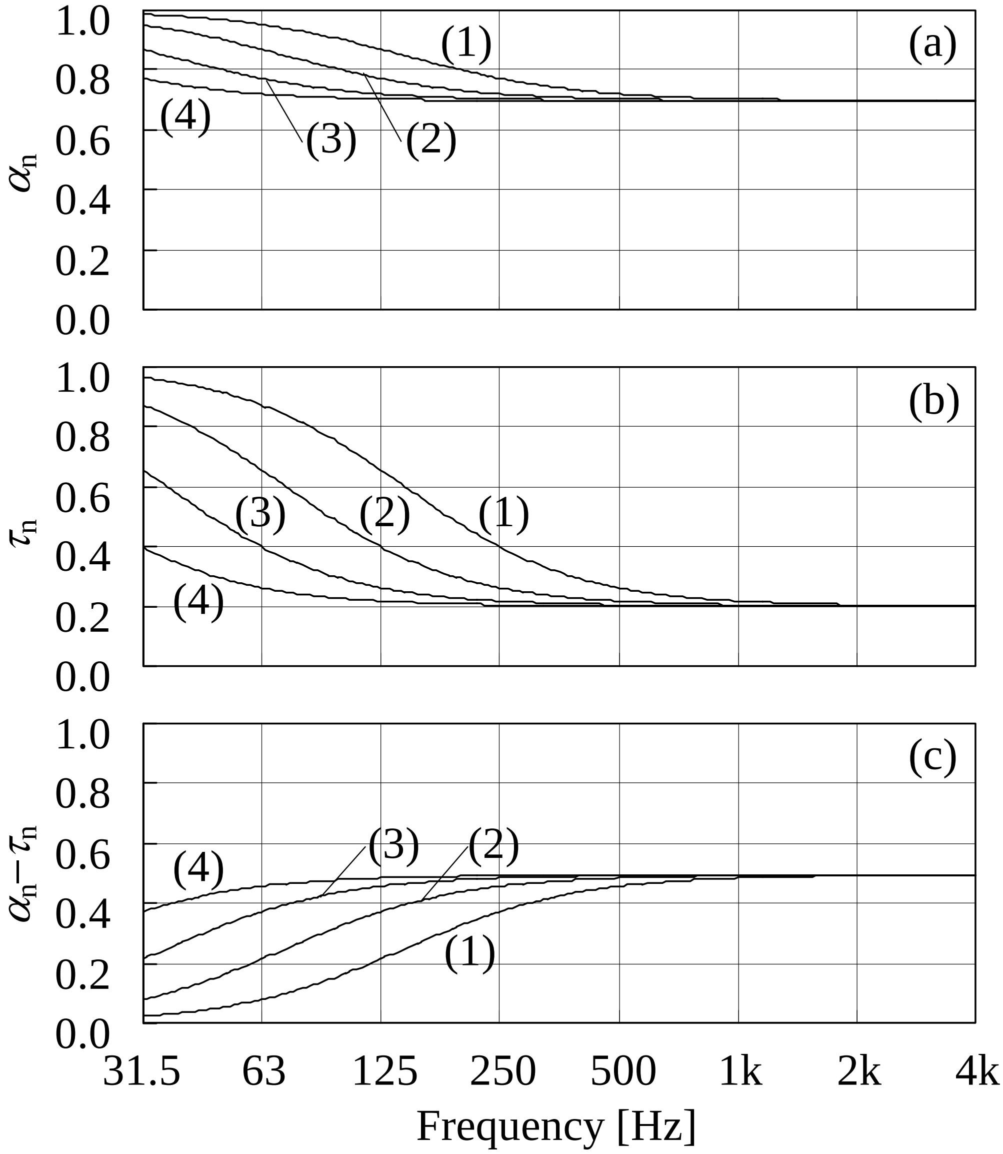

K Sakagami, et al. Detailed analysis of acoustic properties of a permeable membrane

Fig. 3

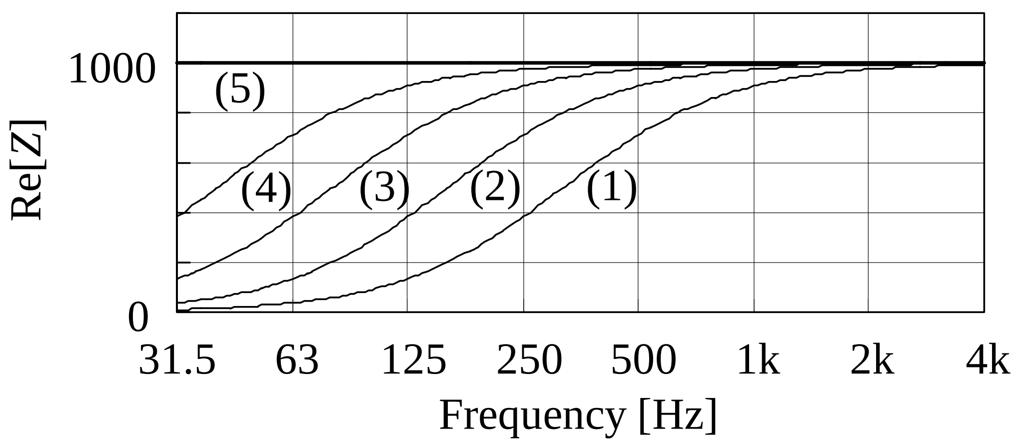

K Sakagami, et al. Detailed analysis of acoustic properties of a permeable membrane

Fig. 4

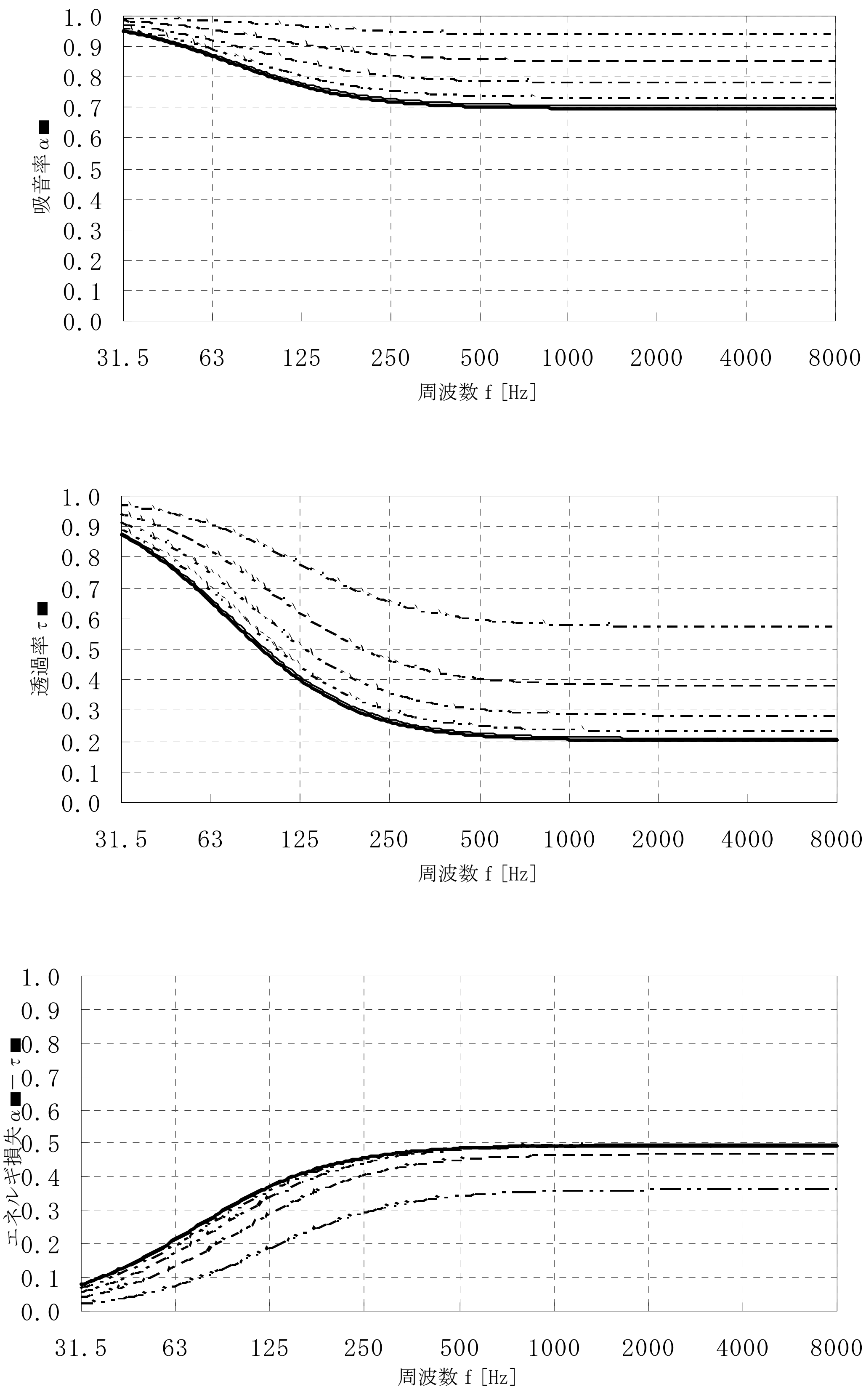

K Sakagami et al. Detailed analysis of ...**Fig. 5**

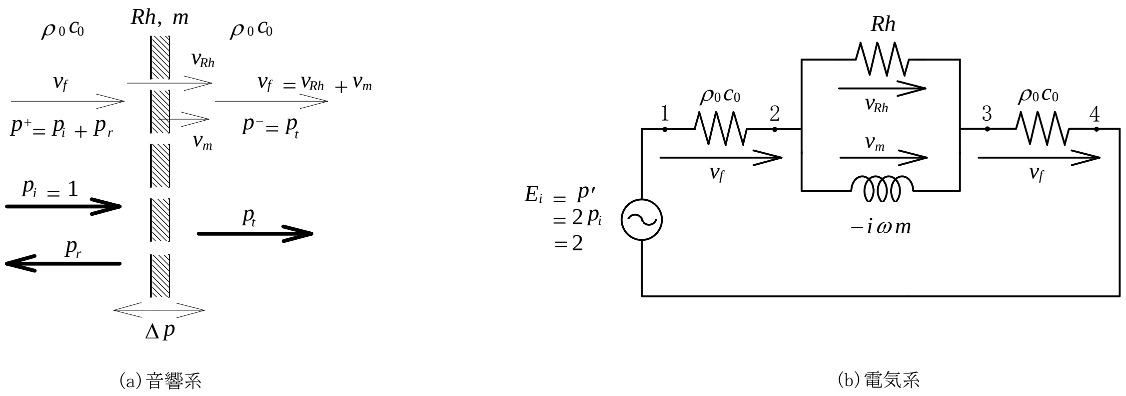

図３．１　(a)解析モデル(音響系)と(b)その等価回路(電気系)

K Sakagami, et al. Detailed analysis of acoustic properties of a permeable membrane

Fig. 6

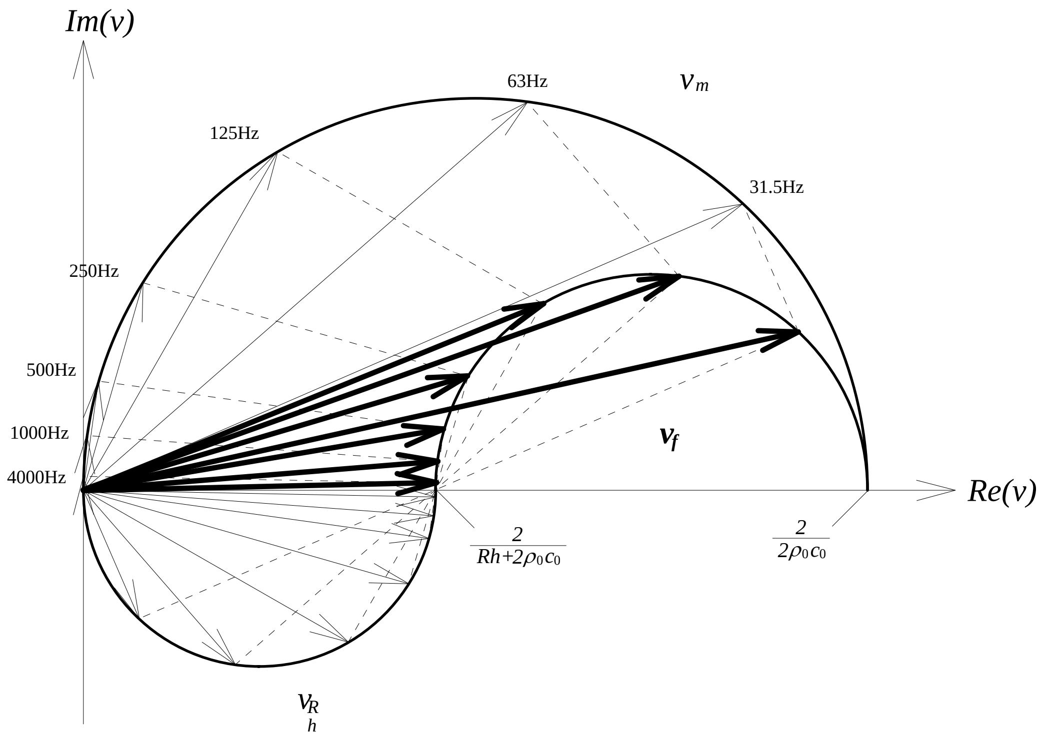

図３．２　複素平面上における粒子速度の変化とその軌跡　(Rh=1000, m=1.0)

K Sakagami, et al. Detailed analysis of acoustic properties of a permeable membrane

Fig. 7

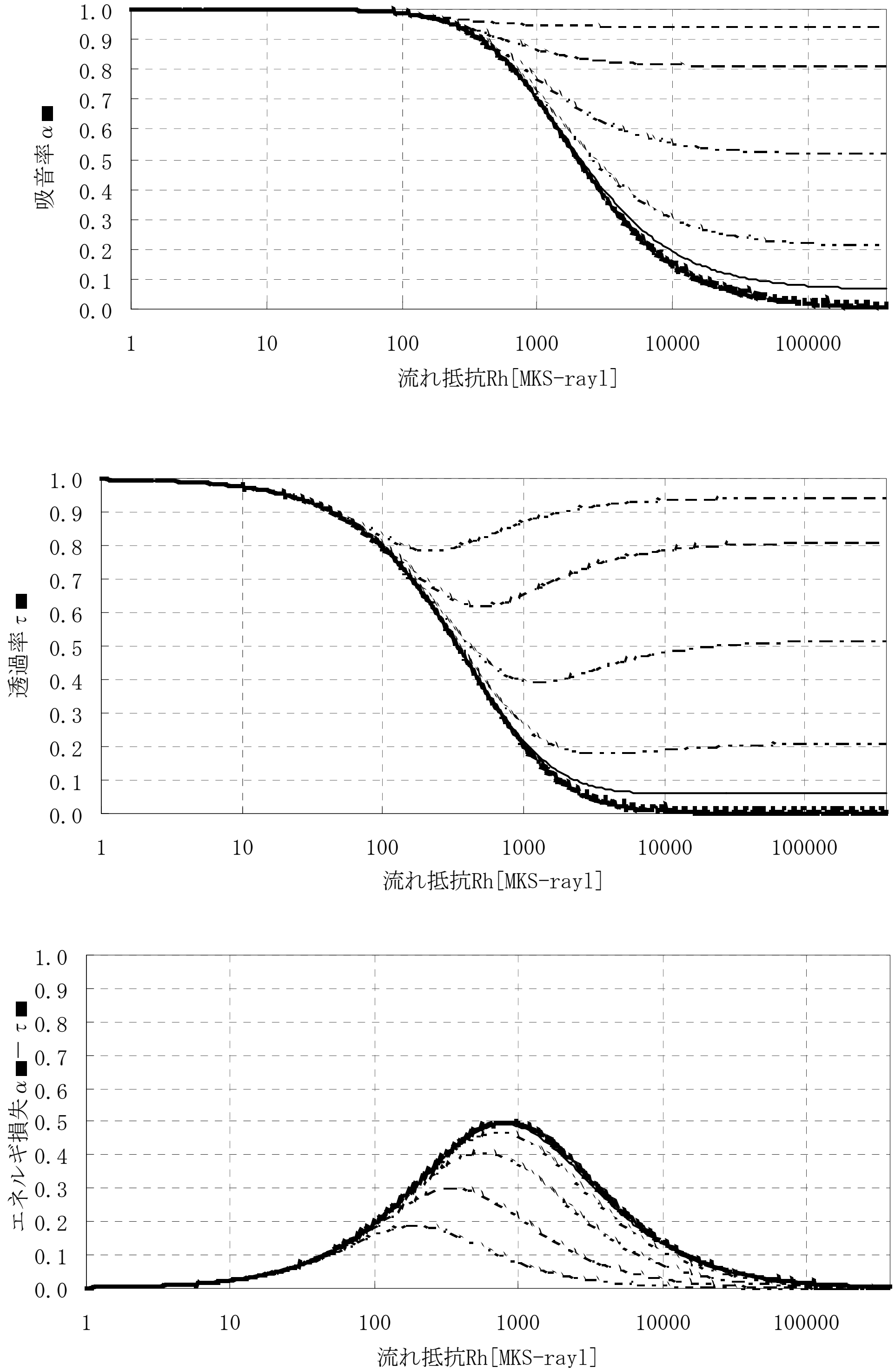

K Sakagami, et al. Detailed analysis of acoustic properties of a permeable membrane **Fig. 8**

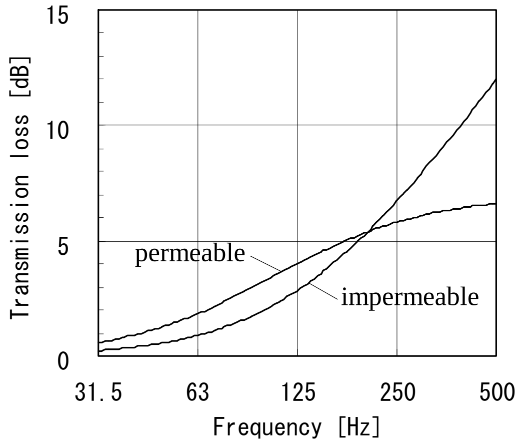

K Sakagami, et al. Detailed analysis of acoustic properties of a permeable membrane

Fig. 9

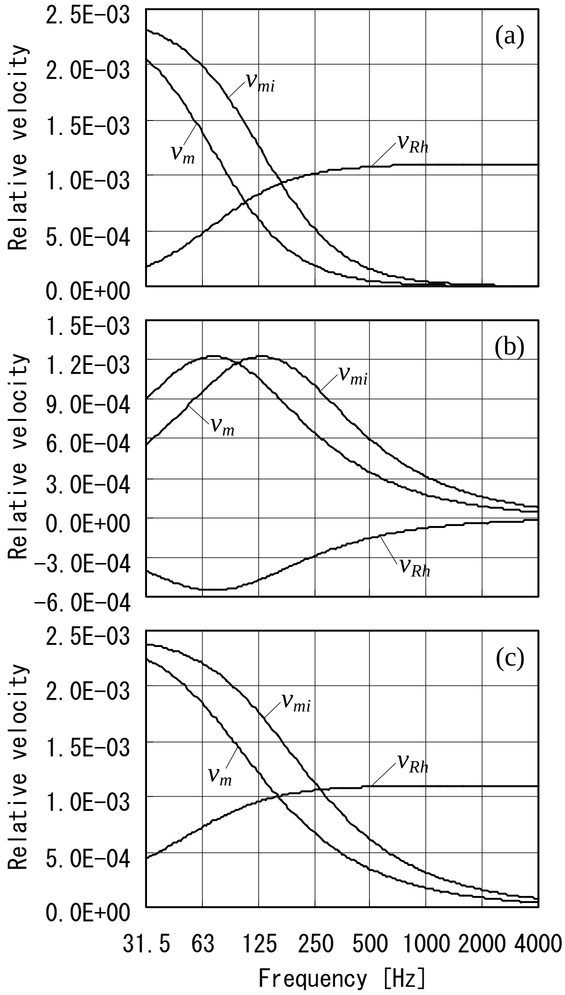

K Sakagami, et al. Detailed analysis of acoustic properties of a permeable membrane

Fig. 10

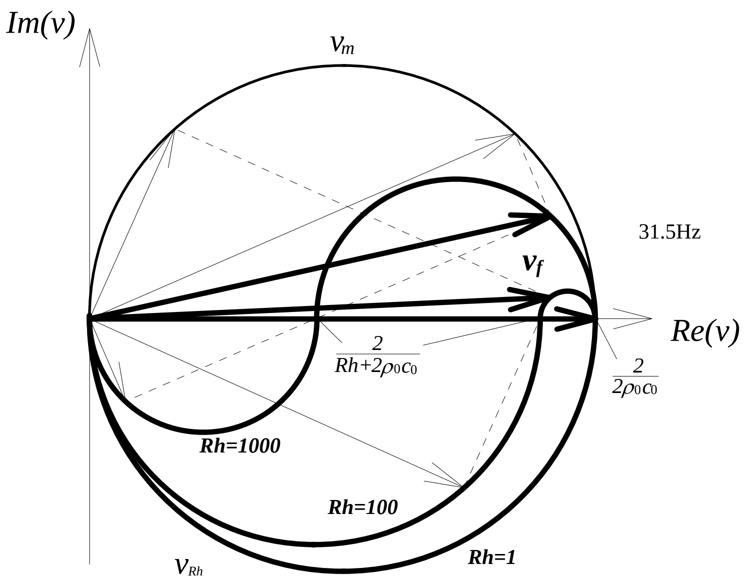

図３．４　流れ抵抗を変化させた場合の粒子速度とその軌跡の変化　*(m=1.0)*

（ベクトルはRh=1, 100, 1000, それぞれの場合の31. 5Hzでの粒子速度）

K Sakagami, et al. Detailed analysis of acoustic properties of a permeable membrane

Fig. 11